The Evolution and Ecology of Virulence in *Xylella fastidiosa*

By

Elise Brooke Woodruff

A thesis submitted to the Graduate Faculty of
Auburn University
in partial fulfillment of the
requirements for the Degree of
Master of Science Entomology

Auburn, Alabama
May 4th, 2024

Keywords: *Xylella fastidiosa*, evolutionary modeling, virulence, microfluidic chamber, biocontrol

Approved by

Nathaniel B Hardy, Chair, Professor of Entomology
Leonardo De La Fuente, Professor of Plant Pathology
Alana Jacobson, Professor of Entomology

ABSTRACT

This thesis investigates the ecology and evolution of virulence in *Xylella fastidiosa*, a xylem-limited bacterium with significant impacts on countless important agricultural plant species. Through microfluidic chamber experiments simulating plant xylem conditions, we assess the potential of *X. fastidiosa* strain EB92-1 to be used as a biocontrol agent against the highly virulent Temecula strain. Our results demonstrate that *Xylella fastidiosa* strain EB92-1 can outcompete a more virulent strain within mixed culture. Additionally, we investigate strain interactions and colonization dynamics in tomato plants, revealing systemic colonization patterns and strain interactions important for developing effective biocontrol strategies. Drawing from individual-based simulation models, we explore the intricate interplay between genetic trade-offs, population structure, and virulence evolution in pathogen populations. We find a general set of conditions in which selection for improved pathogen performance in a vector can cause correlational and potentially maladaptive changes to virulence in the host. This research reveals the complex evolutionary and ecological factors shaping virulence in *X. fastidiosa* and informs future approaches for disease management in agricultural settings.

ACKNOWLEDGEMENTS

I would like to thank my committee for the assistance in the planning and carrying out of my experiments. I would like to thank the Entomology and Plant Pathology Department and The Hardy Lab and the De La Fuente Lab for the funding of my research. I want to express gratitude to my lab mates, Deepak, Noel, Ranlin, Navdeep, Robert, Mamata, Deeksha, and Serena for training me in the necessary lab techniques and always being there to lend a hand. I want to thank Rob Woodruff, Deborah Woodruff, Dr. Gregory Sword, and Cesar Valencia for helping me get my start in the field of science. I express my undying gratitude to my comrades, Billy, Laura, Garrett, and Brittney for their support and companionship throughout my academic career. And I would like to thank Mick for his invaluable service of keeping me sane during the writing of this thesis.

TABLE OF CONTENTS

LIST OF TABLES

LIST OF FIGURES

LIST OF ABBREVIATIONS

- Γ - Deviation from the ideal evolutionary path
- log(T) - log adjusted time value
- N***v*** - number of individuals in vector populations
- Nh- number of individuals in host populations
- ωh - Strength of host selection
- ωv - Strength of vector selection
- mr - migration rate
- V_{max} - maximum virulence effect
- hm – rate of host mortality
- ρ – proportion of host patches
- *k* – strength of pleiotropic covariances
- K_H – carrying capacity of host population
- K_V – carrying capacity of vector population
- CFU – colony forming unit
- EB – EB92-1 strain of *Xylella fastidiosa*
- TM – Temecula strain of *Xylella fastidiosa*
- N_d - number of demes

CHAPTER 1

Introduction

Xylella fastidiosa, a xylem-limited, insect-vectored bacterium, is a significant threat to various plants of agricultural importance, including grapes, olives, citrus, and peach (Johnson et al. 2021, Trkulja et al. 2022, Rapicavoli et al. 2017, Kyrkou et al. 2018). Its pathogenicity derives from its ability to disrupt water and nutrient transport within plants, culminating in symptoms like leaf scorch, wilting, and eventual plant death (Rapicavoli et al. 2017). There is currently no cure for *Xylella fastidiosa*-based diseases, and treatment options are severely limited due to its xylem-limited nature, making it challenging to access and control. Because of this, there is great interest in biocontrol methods, including the use of non-virulent strains of *X. fastidiosa*.

One such strain is EB92-1. EB92-1 is a naturally occurring strain, originally found in elderberry. It is infectious to *Xylella fastidiosa* susceptible plants, however it appears to cause only slight symptoms in hosts (Zhang et al. 2015). An analysis of its genome revealed that it is very similar genetically to the strains causing Pierce's disease in grape. However, EB92-1 is missing 10 genes which are thought to encode secreted pathogenicity factors (Zhang et al. 2011). Previous studies have suggested that it is an efficient biocontrol agent against a more virulent strain, Temecula, in grape (Hopkins 2005), but the mechanisms of this effect are unknown. Additionally, research into the interactions of EB92-1 and Temecula *in vitro* in our lab have not shown this same biocontrol effect.

The conflict between these lines of evidence could stem from the fact that *Xylella fastidiosa* exhibits a high degree of phenotypic plasticity, which aids in its survival in its plant hosts and transmission by insect vectors. Such plasticity can complicate the study of strain interactions in a laboratory setting as the bacteria can behaves quite differently *in*

vitro and *in planta*. Due to the high degree to which *Xylella* can alter its behavior based on experimental conditions, further investigation was required to understand the dynamics of this interaction. We chose to explore the interactions of EB92-1 and Temecula in both a microfluidic chamber to simulate the plant xylem, as well as *in planta* in tomato. We also attempted to investigate insect transmission of this potential biocontrol strain; however, but our efforts were unsuccessful. A complete account of this work can be found in Chapter 2.

In brief, we found that in the microfluidic chamber, the EB92-1 strain consistently out-competes the Temecula strain in terms of growth in both single strain and mixed strain culture. We also found that the growth of Temecula colonies seemed to be inhibited by the EB92-1 strain. This is a positive results in the aim of using EB92-1 as a biocontrol agent. On the other hand, *in planta*, preliminary data suggests that the Temecula strain fares better in terms of growth. However, we reserve judgment until we have more data.

Xylella fastidiosa has complex interactions with both its plant hosts and insect vectors. The theory of virulence evolution, rooted in life history trade-offs within pathogen populations, posits an optimal level of virulence balancing short- and long-term transmission efficiency (Anderson & May 1982; Ewald 1983; Frank 1996: Porco et al. 2005). While short-term transmission efficiency typically increases with within-host pathogen density, excessive virulence leads to host mortality, narrowing the window for pathogen transmission. Consequently, virulence evolution entails a meta-population-level negative feedback, aiming to maximize pathogen transmission over the long term. In the case of *Xylella fastidiosa,* its virulence evolution presents a puzzle. In some cases, *Xylella* populations express virulence phenotypes that would seem non-adaptive (Redak et al. 2004), as plants that are heavily infected are in some cases avoided by vectors (Daugherty et al. 2011). One factor that could be driving this potentially non-adaptive virulence is antagonistic pleiotropy between traits affecting performance in the host and the vector. Transmission of

Xylella fastidiosa is boosted when cells express phenotypes which produce more EPS along with other virulence factors affecting insect retention. However, this expression also increases the extent to which they harm their host plant (Killiny et al. 2013). The emergence of highly virulent phenotypes in specific host-pathogen interactions, such as grapevine infections coinciding with the spread of the glassy-winged sharpshooter (Hemiptera: Cicadellidae*: Homalodisca vitripennis*) vector in California, suggests a complex interplay between pathogen evolution and vector dynamics. In comparison to many resident species of xylem-feeding insects, *H. vitripennis* is an inefficient vector of *X. fastidiosa* (Bextine 2006, Redak 2004). But as it established in California, it became so numerically dominant that most transmission to and from grapevine in California is now via *H. vitripennis*. With this establishment of the vector, came new highly virulent phenotypes. Given the complex ecology of Xf, including its association with a wide range of host species highlights its versatility, ranging from benign commensalism to highly virulent infections, it is not clear if selection in the vector actually could drive the evolution of phenotypes that are expressed in a host.

To improve our intuition about how genetic architecture and environmental heterogeneity interact to shape the course of the evolution of virulence, we develop and analyze an individual-based simulation model. An account of this work can be found in Chapter 3. We found that, if there is strong negative pleiotropy, selection in the vector can indeed drive much correlational evolution in the host. However, this depends on a variety of other factors such as the relative abundance and carrying capacities of hosts and vectors.

So, through a combination of experimental studies and computational simulations, we aim to shed light on the ecology and evolution of virulence in *X. fastidiosa* and explore potential biocontrol solutions. With this we hope to set the stage for the development of effective strategies for *Xylella fastidiosa* control in agricultural settings.

1.1 REFERENCES

Anderson RM, May RM. Directly transmitted infectious diseases: control by vaccination. Science. 1982 Feb 26;215(4536):1053-60. doi: 10.1126/science.7063839. PMID: 7063839.

Bextine, Blake, Brian C Jackson, and Matthew J Blua. Quantitative aspects of the transmission of xylella fastidiosa by the ..., 2006. https://static.cdfa.ca.gov/PiercesDisease/proceedings/2006/2006_13-17.pdf.

Daugherty, M.P., Rashed, A., Almeida, R.P.P. and Perring, T.M. (2011), Vector preference for hosts differing in infection status: sharpshooter movement and *Xylella fastidiosa* transmission. Ecological Entomology, 36: 654-662. https://doi.org/10.1111/j.1365-2311.2011.01309.x

Ebert D, Mangin KL. THE INFLUENCE OF HOST DEMOGRAPHY ON THE EVOLUTION OF VIRULENCE OF A MICROSPORIDIAN GUT PARASITE. Evolution. 1997 Dec;51(6):1828-1837. doi: 10.1111/j.1558-5646.1997.tb05106.x. PMID: 28565099.

Ebert, 1994. Evolution of infectious disease. Oxford University Press, New York, New York, 298 p. 36

Frank SA. Models of parasite virulence. Q Rev Biol. 1996 Mar;71(1):37-78. doi: 10.1086/419267. PMID: 8919665

Hopkins DL. Biological Control of Pierce's Disease in the Vineyard with Strains of Xylella fastidiosa Benign to Grapevine. Plant Dis. 2005 Dec;89(12):1348-1352. doi: 10.1094/PD-89-1348. PMID: 30791315.

Johnson, K.A., Bock, C.H. & Brannen, P.M. Phony peach disease: past and present impact on the peach industry in the southeastern U.S.A. CABI Agric Biosci 2, 29 (2021). https://doi.org/10.1186/s43170-021-00049-4

Killiny N, Martinez RH, Dumenyo CK, Cooksey DA, Almeida RP. The exopolysaccharide of Xylella fastidiosa is essential for biofilm formation, plant virulence, and vector transmission. Mol Plant Microbe Interact. 2013 Sep;26(9):1044-53. doi: 10.1094/MPMI-09-12-0211-R. PMID: 23678891.

Kyrkou I, Pusa T, Ellegaard-Jensen L, Sagot MF, Hansen LH. Pierce's Disease of Grapevines: A Review of Control Strategies and an Outline of an Epidemiological Model. Front Microbiol. 2018 Sep 12;9:2141. doi: 10.3389/fmicb.2018.02141. PMID: 30258423; PMCID: PMC6143690.

Porco TC, Lloyd-Smith JO, Gross KL, Galvani AP. The effect of treatment on pathogen virulence. J Theor Biol. 2005 Mar 7;233(1):91-102. doi: 10.1016/j.jtbi.2004.09.009. Epub 2004 Nov 13. PMID: 15615623; PMCID: PMC7126720.

Rapicavoli, J., Ingel, B., Blanco-Ulate, B., Cantu, D. and Roper, C. (2018), Xylella fastidiosa: an examination of a re-emerging plant pathogen†. Molecular Plant Pathology, 19: 786-800. https://doi.org/10.1111/mpp.12585

Redak, R.A., Prucell, A.H., Lopes, J.R.S., Blua, M.J., Mizell III, R.F., and P.C. Andersen. 2004. The biology of xylem fluid-feeding insect vectors of Xylella fastidiosa and their relation to disease epidemiology. Annu. Rev. Entomol. 49:243-270.

Trkulja V, Tomić A, Iličić R, Nožinić M, Milovanović TP. Xylella fastidiosa in Europe: From the Introduction to the Current Status. Plant Pathol J. 2022 Dec;38(6):551-571. doi: 10.5423/PPJ.RW.09.2022.0127. Epub 2022 Dec 1. PMID: 36503185; PMCID: PMC9742796.

Zhang S, Flores-Cruz Z, Kumar D, Chakrabarty P, Hopkins DL, Gabriel DW 2011. The Xylella fastidiosa Biocontrol Strain EB92-1 Genome Is Very Similar and Syntenic to Pierce's Disease Strains. J Bacteriol 193:. https://doi.org/10.1128/jb.05430-11

CHAPTER 2

Interactions Between Xylella *fastidiosa* strains EB92-1 and Temecula

2.1 ABSTRACT

Xylella fastidiosa, a xylem-limited bacteria, poses significant threats to various plant species of agricultural importance, causing diseases like Pierce's disease and citrus variegated chlorosis. This study evaluates the potential of *X. fastidiosa* strain EB92-1 as a biocontrol agent against the highly virulent Temecula strain using microfluidic chambers, which simulate plant xylem conditions, as well as in tomato. Additionally, we attempted to develop a protocol for an artificial diet transmission system for our vectors. Our results demonstrate consistent and significant out-competition of Temecula by EB92-1 in mixed culture within microfluidic chambers. These findings suggest that EB92-1 has potential efficacy as a biocontrol agent against *X. fastidiosa*-associated diseases. Our results for the tomato and artificial diet system were inconclusive and indicate the need for further study of this system.

2.2 INTRODUCTION

Field studies have indicated that infection of grapevine by EB92-1 may confer on plants protection against virulent strains of *Xylella* (Hopkins 2005). Over a 30+ period, prior infection with the EB92-1 strain significantly lowered disease severity in plants later infected with a virulent strain of *X. fastidiosa*. Likewise, in a related study, EB92-1 was used to mitigate the effects of Huanglongbing (HLB) caused by *Candidatus Liberibacter* asiaticus. The EB92-1 strain was shown to colonize citrus and decrease the incidence of

symptomatic trees as well as the percentage of trees seen with severe symptoms (Hopkins, Ager 2021). However, the mechanisms of this protection are unknown.

X. fastidiosa exhibits a high degree of phenotypic plasticity, which aids in its survival in its plant hosts and transmission by insect vectors. However, this plasticity complicates the study of strain interactions in a laboratory setting as the bacteria can behave quite differently *in vitro* and *in planta*. As the name suggests, *Xylella fastidiosa* exhibits fastidious growth, and can be very sensitive to changes in environment or content of growth media. Previous research in the De La Fuente lab examined the interactions between the Temecula and EB92-1 lines in a 96 well plate. In that in vitro setting, EB92-1 did not appear to hinder the growth of Temecula. However, due to the high degree to which *Xylella* can alter its behavior based on the local environment, further investigation was required to understand the dynamics of this interaction, particularly in environments that more closely mimic the natural habitat of *X. fastidiosa*. Therefore, our goals for this study were to characterize the population dynamic interactions between EB92-1 and Temecula in (1) microfluidic chambers, (2) in planta, and (3) in vectors.

Microfluidic chambers simulate the conditions within plant xylem, while also making what happens in such an environment easier to observe. They offer constant flows of media and nutrients, through fine channels, of approximately the same diameter as xylem vessels.

For our *in-planta* assays, we used tomato as a model system. Previous research in the De La Fuente lab showed that tomato plants could be systemically, but asymptomatically colonized by the Temecula strain of *X. fastidiosa* (Chen et al. 2017). So, the advantages of using tomato as a model, are that it is a viable host that is easy to cultivate and does not become ill when infected. Moreover, tomato also has the potential to be used for deployment of biocontrol strains in the field.

For our in-vector assays, we attempted to use insects from a colony established from a local population of *Homalodisca vitripennis*, the glassy-winged sharpshooter. Ultimately this line of research was unsuccessful. But here we provide a description of our culturing methods and assay designs, to help future researchers.

2.3 METHODS

2.3.1 Microfluidic chamber experiment

The strains of *X. fastidiosa* used in this experiment were Temecula and EB92-1. Each has been previously transformed to carry an antibiotic resistance cassette. Specifically, EB92-1 was transformed to be Kanamycin resistant, and Temecula was transformed to resist Chloramphenicol. Use of these transformed stained allowed for quantification of experimental strain densities via plating on antibiotic media.

The chloramphenicol-resistant Temecula strain and the kanamycin-resistant EB92-1 strain, were grown on PW plates from glycerol stock. These initial plates were grown for approximately 7 days. The bacteria was then scraped off the plates, streaked onto new plates, and allowed to grow for another 7 days. Then, using a sterile inoculation loop, bacteria were collected from plates wand transferred into the test tubes containing PD2 media. The suspension was then homogenized using a pipette to evenly distribute the bacteria without inducing bubble formation. A blank control was established by filling a separate test tube with 1 ml of media. Spectrophotometer measurements were conducted at 600nm wavelength after agitating each suspension to prevent bacterial settling. Each bacterial suspension was then adjusted to an OD_{600} of 0.60.

The mixed strain culture was prepared by adding equal parts of the adjusted EB92-1 and Temecula-L suspensions into an empty test tube and vortexing to combine.

2.3.1a Chamber Assembly:

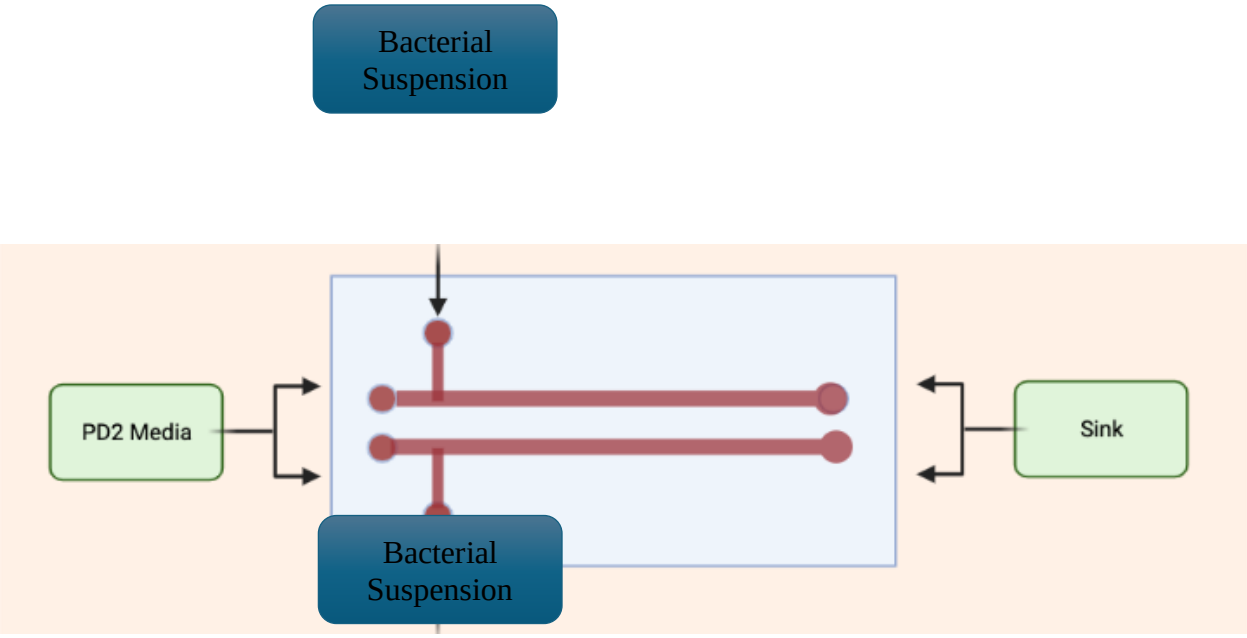

Fig. 2.1: General setup of one microfluidic unit, containing two individual microfluidic chambers

Outlet syringes were prepared by removing the plungers from two 5 ml syringes and attaching them to tubes labeled "Sink." These syringes were used to catch the media pushed out of the chamber, and along with it, the planktonic bacteria which did not attach to the chamber walls. Sterile cotton balls were inserted into the syringe tops to block the tubes. Media inlets were prepared by drawing 5 ml of media into syringes, removing bubbles, and attaching them to the chamber. Similarly, adjusted bacterial solutions were drawn into 1 ml syringes, bubbles were removed, and syringes were attached to the chamber. Priming the chamber involved gently pushing media through to remove air bubbles.

2.3.1b Experimental Setup:

The NIS-Elements software (Nikon Corporation – Tokyo, Japan) was used to monitor chamber conditions under the view of the microscope. Bacterial flow was set to 2-5 ul/min to clear remaining air from the tubing until reaching the chamber. Media flow was also set to 2-5 ul/min to clear bubbles, with speeds reduced to 500 nl/min when air began to clear from the chamber. Flow rates were adjusted throughout the process to maintain bubble-free conditions. Once no bubbles were observed, media flow was reduced to 250-275 nl/min, and bacterial flow was adjusted to 250-400 nl/min based on experimental needs. Upon achieving sufficient bacterial presence in both chambers (Fig. 2.2), the bacterial pump was turned off, and bacterial tubing was clamped to prevent bubble entry. Media flow was maintained at 250-275 nl/min for the duration of the experiment.

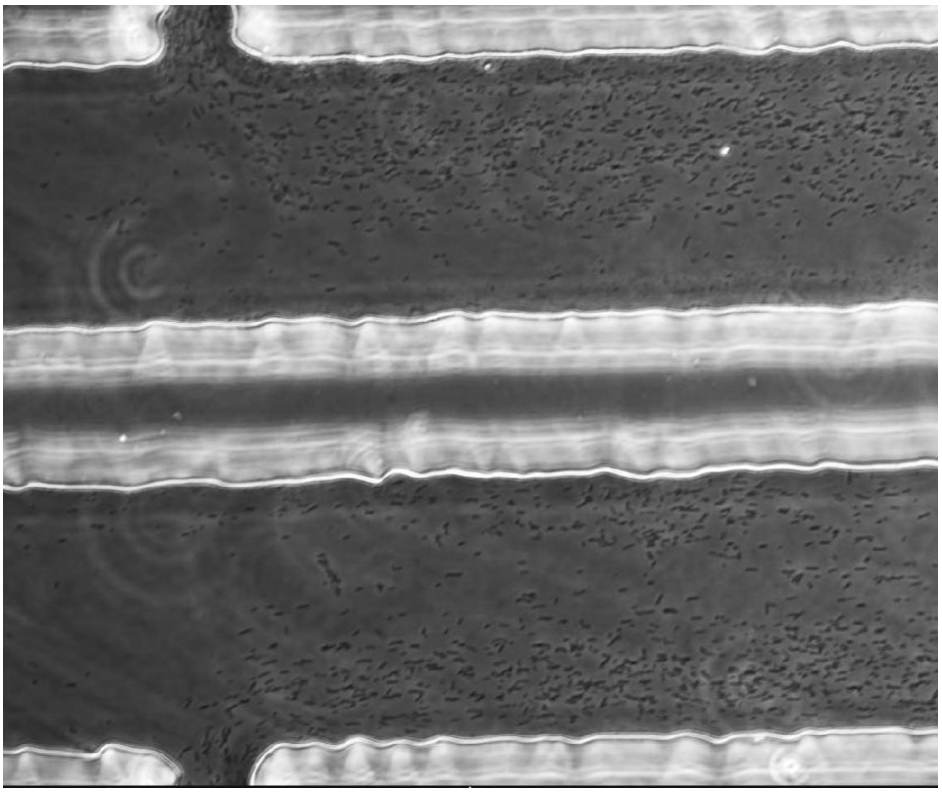

Fig. 2.2: Bacterial cells forming attachment to microfluidic chamber walls.

Four individual treatments were run for each of the trials: the Temecula only control, the EB92-1 only control, and two individual mixed strain chambers. Two trials were performed, resulting in 4 replicates of the mixed strain culture treatment.

The trials were run for 10 days at a media flow rate of 0.25 µl min^{-1} and samples were taken from both the outlet syringe as well as the biofilm formation of each chamber, which was pushed out via increase of flow rate. Cells in the suspension were enumerated by plating serially diluted samples onto PW agar, then incubated for 14 days. After this incubation period, colony forming units were counted and these results were quantified.

2.3.2 *In Planta* Experiment

Our two strains, kanamycin resistant EB92-1 and chloramphenicol resistant Temecula were grown on their respective antibiotic PW (periwinkle wilt) media for 7 days, then streaked onto new plates and grown for an additional 7 days. The bacteria were then scraped off the plates and suspended in succinate-citrate-phosphate (SCP) buffer at OD600 of 1.0 prior to inoculation, as previously described (De La Fuente et al., 2013). Four treatments were used, the buffer only control, the Temecula only treatment, the EB92-1 only treatment, and the mixed strain treatment. Each of these treatments had 10 replicate plants.

Plants were inoculated using the pin-prick method as described in De La Fuente et al. (2013). The inoculation point was at the stem attached to the first true leaf pair. At the inoculation point, each plant was probed six times by a 1 ml tuberculin syringe with a 23-gauge needle, and 100 µl inoculum were used. After inoculation, plants were placed into a randomized block design.

Samples were taken at 15, 45, and 90 days. For these samples, leaf petiole tissue was taken from 3 plants per treatment at each sampling date. Petioles from the 2nd, 3rd, and 5th true leaf were taken at each sampling date, and surface sterilized using the protocol outlined in Chen et al. (2017). The petioles were then finely chopped and introduced in test tubes containing PD2 broth and incubated at 28 ℃ with shaking at 150 rpm for 1 h. The supernatant was serially diluted and spread-plated onto PW plates.

2.3.3 Insect Vector Transmission Experiment

The *X. fastidiosa* strains Temecula and EB92-1 were initially cultured on PW medium for 7 days, followed by streaking onto XFM-pectin medium for approximately 10 days.

Subsequently, each strain was suspended in an artificial diet solution as described by Killiny (2009), comprising L-glutamine 0.7 mM, L-asparagine 0.1 mM, and 1 mM sodium citrate, adjusted to pH 6.4, and then adjusted to an optical density at 600 nm (OD600) of 0.4, following the protocol by Rashed (2010).

The artificial diet chambers were assembled using 50 mL Falcon tubes with the closed end removed, leaving one open end and one capped end. The open end of each chamber was covered with a thin layer of parafilm onto which 500 microliters of the bacterial suspension was placed. The suspension was then covered with an additional layer of parafilm to form a closed sachet, following modifications from Killiny (2009). An image of the experimental setup can be seen in Figure 2.3 below. Assembly of the chambers was conducted under a laminar flow hood to prevent contamination of the diet solution.

Fig. 2.3: The chambers in which the artificial diet acquisition and transmission studies were conducted.

A laboratory population of glassy winged sharpshooters was initiated from field collected insects from Auburn, Alabama. Pre-experiment, these insects were maintained in two tent-shaped, 60 cm × 60 cm × 60 cm bugdorms (BioQuip, Rancho Dominquez, CA, USA). Insects were reared on a diet of sunflower, okra, periwinkle, tomato, and basil plants. The insects used for each replicate were reared on basil plants for a week prior to the experiment to ensure uniform conditions. They were then placed into the chambers and allowed to feed on the diet solution for a 24-hour acquisition period.

Following acquisition, the parafilm feeding sachet was replaced with a sachet containing only 1 mL of artificial diet solution, and the insects were allowed to feed for an inoculation access period of 24 hours.

Afterward, each insect was removed from the chamber, decapitated, and the heads homogenized into 1 ml of PD2 media using a small pestle as per Almeida and Purcell (2003). This solution was then used for serial dilution plating as was described in previous sections. The remaining diet solution in the sachet was also collected used for serial dilution plating. From these samples we took CFU counts to determine bacterial ratios. Each replicate consisted of 20 total diet chambers, with 10 containing the Temecula strain and 10 containing the EB92-1 strain.

Four replicates were intended to be performed in 2–3-week intervals to avoid depleting the colony of Glassy-winged Sharpshooter adults and to allow sufficient time for bacterial growth. However, due to challenges in the study (see discussion section) only one replicate was completed.

2.4 RESULTS AND DISCUSSION

2.4.1 Microfluidic chamber experiment

We found that the EB92-1 strain consistently outperformed the Temecula strain. It appears that the EB92-1 strain is better able to colonize the mock xylem of our model system; there were significantly more EB92-1 colonies, both in mixed-culture chambers as well as in the single strain controls. (Fig. 2.4). In the mixed culture treatments, we found that that the abundance of both strains was diminished, indicating some form of antagonism (Fig. 2.4).

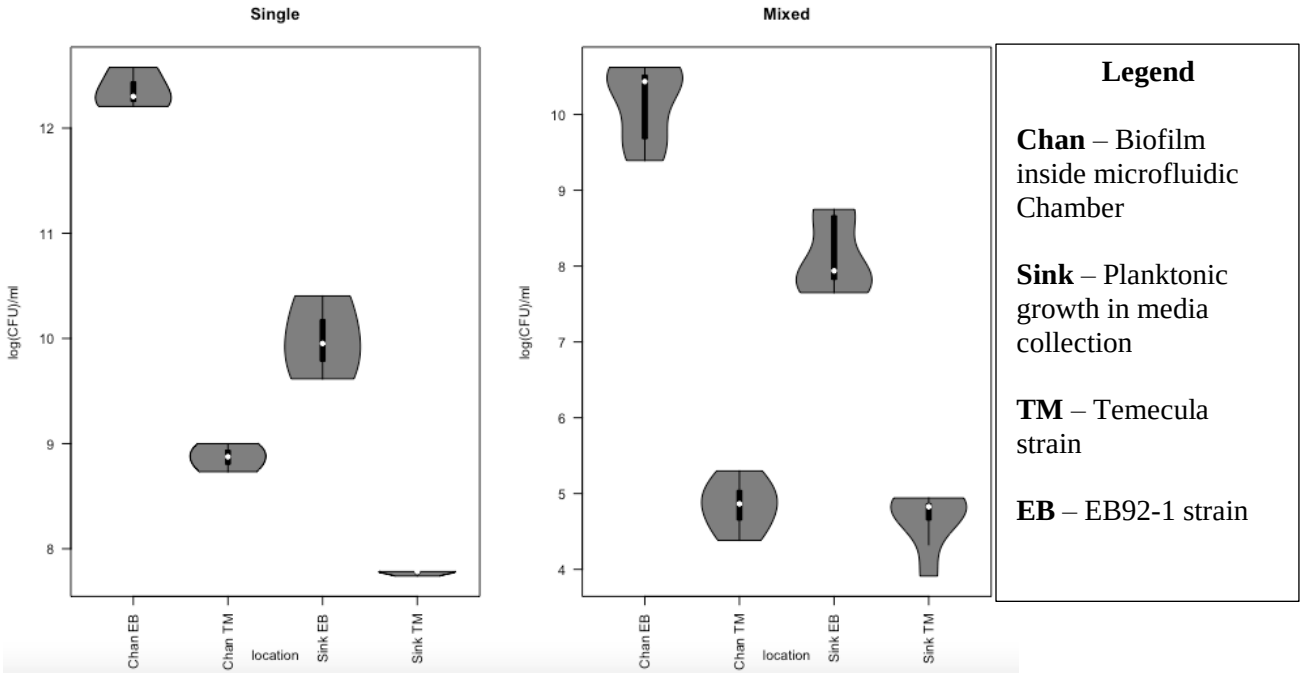

Fig. 2.4: Results of the single and mixed strain Log(CFU)/ml counts for microfluidic chamber, sorted by location.

Tukey multiple comparisons of means were performed for both the single and mixed strain treatment groups. For the single strain, each of the comparisons of mean CFU values were significantly different (p value < 0.05) except for the comparison between the Temecula strain in the sink environment and the Temecula strain in the channel environment (p value = 0.881). For the mixed treatment, the mean CFU count values were scaled by the mean CFU values in the single strain treatments. We found that there were significantly more of the EB92-1 strain than the Temecula strain in both the channel (p value = 0.00767) and the sink (p value = 0.00221).

Additionally, when we look at the proportional change in CFU counts brought about by mixing for each strain, we find that the Temecula strain has a higher level of decrease than the EB92-1 in mixed culture (Fig. 2.5).

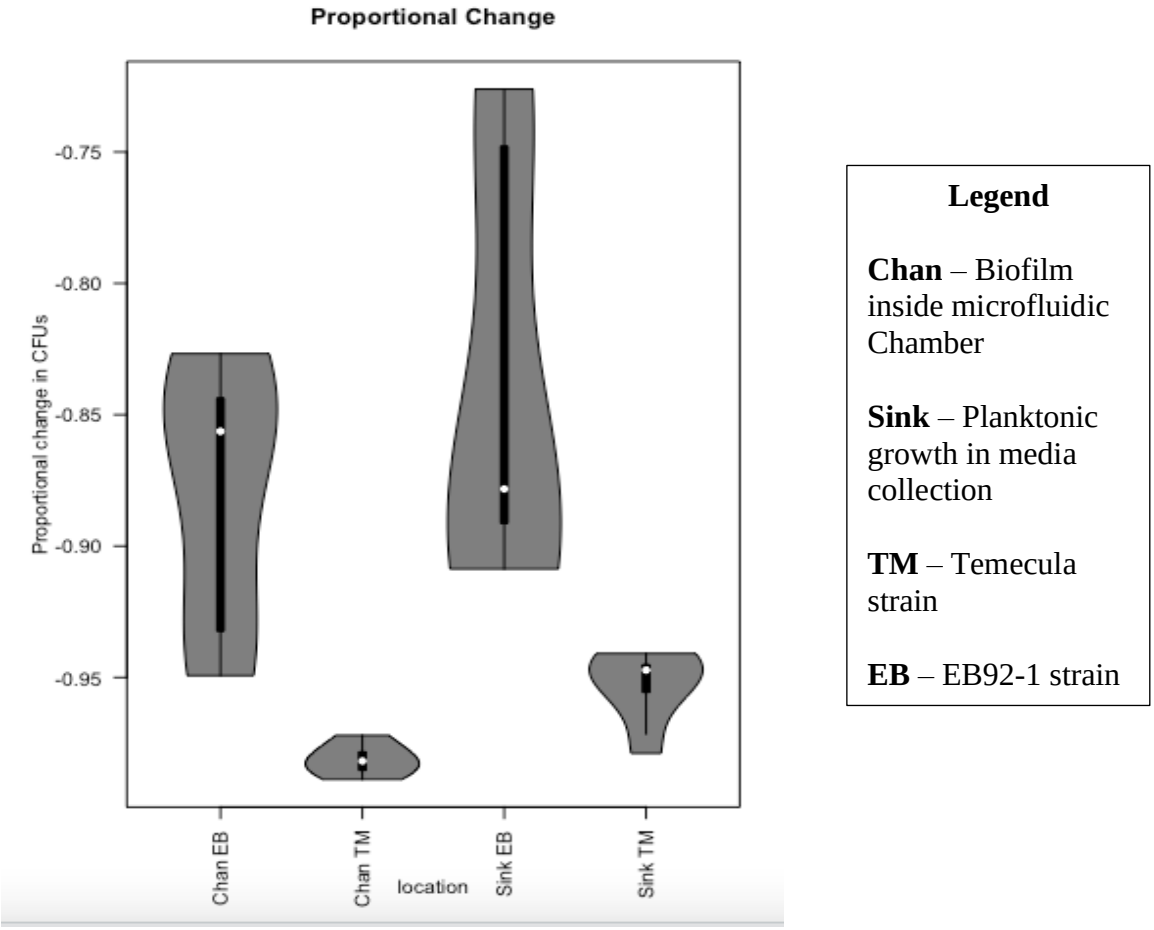

Fig. 2.5: Percent change in abundance of colony forming units for each of the strains between the single strain and mixed strain treatments, sorted by location.

So, the performance of both strains is decreased in mixed cultures. But the antagonistic effects are asymmetrical; expose to EB92-1 much more drastically inhibits the growth of Temecula colonies than vice versa.

The population dynamic interactions observed between *X. fastidiosa* strains EB92-1 and Temecula in mixed culture biofilms align with previous research indicating strain-specific interactions within microbial communities (Vandenkoornhuyse et al., 2002). The dominance of EB92-1 in both single and mixed culture settings suggests a superior ability

to colonize and establish within the mock xylem environment. This competitive advantage is consistent with findings in other pathogenic systems, where certain strains exhibit enhanced fitness in colonization and resource utilization (Trivedi et al., 2020).
The observed antagonistic dynamics between EB92-1 and Temecula, resulting in decreased abundance of both strains upon mixing, resonate with studies on interspecies competition within biofilm communities (Pande et al., 2016). Such interactions often involve resource competition, metabolic interactions, and production of antimicrobial compounds, all of which influence the composition and stability of microbial consortia (Hibbing et al., 2010). The more pronounced inhibition of Temecula suggests a potential susceptibility to competition-induced stress or inhibition by EB92-1, indicating strain-specific responses to environmental cues and interspecific interactions (Wei et al., 2019).

The concept of using non-virulent or attenuated strains as biocontrol agents against pathogenic microbes has gained traction in recent years (Wu et al., 2021). By out-competing and displacing virulent strains, biocontrol strains like EB92-1 disrupt disease progression and reduce pathogen load in host plants. This approach leverages ecological principles to manipulate microbial communities and mitigate disease incidence, offering a sustainable alternative to chemical pesticides (Raaijmakers et al., 2009).

2.4.2 In planta experimentation

From the 15-day time point we found that both strains appear to be systemically colonizing the tomato plants in both single and mixed strain culture, with bacteria being found in all sampling groups from 2nd to 5th true leaf. For the single strain treatments, our two strains, EB92-1 and Temecula, appear to be colonizing the plants in relatively similar amounts (Fig. 2.6).

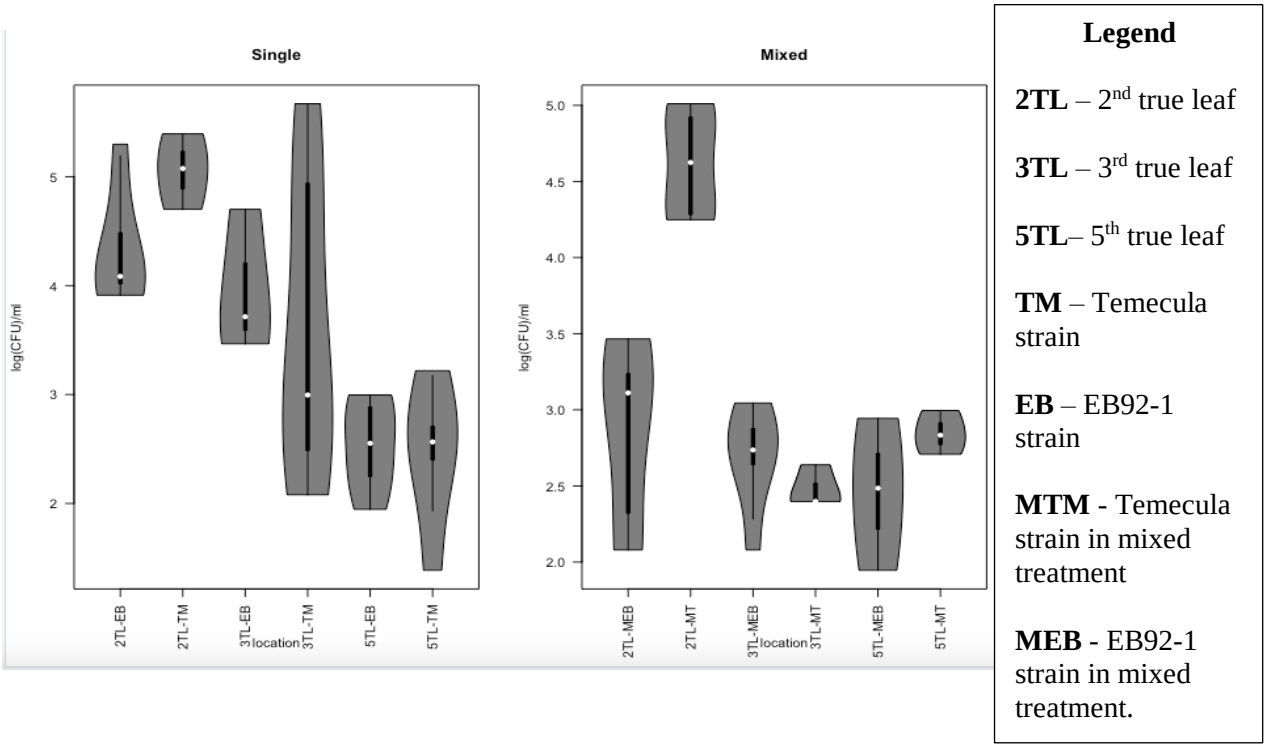

Fig. 2.6: L: single strain treatments of Temecula and EB92-1 at 2nd, 3rd, and 5th true leaf. R: Mixed strain treatments of Temecula and EB92-1 at 2nd, 3rd, and 5th true leaf. Both quantified in Log(CFU)/ml.

From the mixed strain treatment, we can see that it does initially appear that the Temecula strain is colonizing the lowest region of the plant in higher amounts than the EB92-1 strain (p value = 0.0134016). However, this result may not be representative of the true colonization as contamination issues led to a much smaller sampling size for this data. This result will be reevaluated at later sampling dates.

2.4.3 Insect transmission experimentation

We aimed to establish an artificial diet transmission system to inoculate insects with *Xylella* and assess transmission rates. We tried follow aa protocol developed for Blue green sharpshooter (BGSS) (Killiny et al., 2009), but this proved unsuitable due to the more discerning feeding habits of the Glassy-winged sharpshooter (GWSS) . Despite efforts to enhance feeding efficiency, the insects were reluctant to feed on the artificial diet. Many of the insects perished in the chambers rather than feeding on the artificial diet solution.

Successful transmission of *Xylella* by the insect vectors necessitated growing the bacteria in minimal media in order to trigger the DSF pathway for colonization (Newman et al. 2004). For this study XFM media with pectin was used, as in (Killiny et al. 2009) However, cultivating *Xylella* on such media presented challenges due to its finicky nature and slow growth rate. The limited bacterial yield impeded the progression of experiments.

Compounding these challenges, we had issues with contamination. A non-target bacterium proliferated rapidly on the kanamycin plates, which obscured Xylella growth and made it impossible to accurately count colony-forming units (CFU) . It is likely that an error in media preparation allowed for the growth of this bacteria on the antibiotic plates.

Additionally, efforts to maintain the GWSS colony and prevent diapause through light-dark cycle adjustments proved insufficient, leading to a decline in colony levels below what was needed for experiments. Ultimately, time constraints curtailed further attempts to overcome these obstacles, preventing the completion of the planned insect- transmission study.

2.5 CONCLUSIONS

The microfluidic chamber study lends further credence to the potential of using the EB92-1 strain as a biocontrol agent against the virulent Temecula strain. In microfluidic chambers, we observed consistent and significant inhibition of Temecula by EB92-1. The fact that the Temecula strain is more inhibited by EB92-1 than vice versa is especially encouraging. The observed success of EB92-1 in outcompeting Temecula within the microfluidic chamber contrasts with previous findings from studies conducted in different experimental setups, such as 96-well plates. This discrepancy underscores the importance of studying bacterial interactions in environments that closely mimic the natural habitat, especially for species such as *X. fastidiosa* which are known to be highly phenotypically platic. Further research into the mechanisms underlying the antagonistic interactions between EB92-1 and Temecula, as well as their implications for biofilm formation and resource competition within the plant xylem, will be crucial for optimizing the use EB92-1 as a biocontrol agent in agricultural settings.

For the in-planta experiments, samples have yet to be taken for the 45 and 90 day post inoculation points. When these samples are taken, this data will be added to the manuscript and final conclusions will be made. So, further research is needed to more accurately characterize the colonization (and transmission) dynamics of *Xylella* strains in planta. However, our preliminary results further highlight the extensive context dependency and complexity of Xylella ecology.

Our efforts to study variation in insect transmission efficiency across strains of *Xylella* were unsuccessful. But the the ability of EB92-1 to be spread effectively by vectors of *Xylella fastidiosa* would be an important consideration for its use in biocontrol. Hence,

further research along this line will be valuable. We hope that our failures help others to succeed.

In conclusion, our micro-fluidics experiment lends further support for the potential of using EB92-1 as a biocontrol strain to protect plant from more virulent strains of *Xylella*. Our preliminary observations of the interactions between strains in tomato would seem to provide evidence to the contrary, but that experiment is not yet complete, and so we cannot be sure how things will unfold. Regardless, every indication is that what happens between two strains of *Xylella* depends strongly on the context, and so experiments in other host plant species will be essential, as will be research into the specific molecular mechanisms of the interactions between strains and their hosts.

2.6 REFERENCES

Almeida, R. P. P., & Lindow, S. (2008). Living in two worlds: the plant and insect lifestyles of Xylella fastidiosa. Annual Review of Phytopathology, 46, 243-271.

Almeida, R. P. P., & Purcell, A. H. (2003). Transmission of Xylella fastidiosa to Grapevines by Homalodisca coagulata (Hemiptera: Cicadellidae). Journal of Economic Entomology, 96(2), 264-271. https://doi.org/10.1093/jee/96.2.264

Chen, H., Kandel, P. P., Cruz, L. F., Cobine, P. A., & De La Fuente, L. (2017). The major outer membrane protein MopB is required for twitching movement and affects biofilm formation and virulence in two Xylella fastidiosa strains. Molecular Plant-Microbe Interactions, 30, 896-905.

Chatterjee, S., Almeida, R. P. P., & Lindow, S. (2008). Living in two worlds: the plant and insect lifestyles of Xylella fastidiosa. Annual Review of Phytopathology, 46, 243-271.

Hibbing, M. E., Fuqua, C., Parsek, M. R., & Peterson, S. B. (2010). Bacterial competition: surviving and thriving in the microbial jungle. Nature Reviews Microbiology, 8(1), 15-25.

Hopkins, D. L. (2005). Biological Control of Pierce's Disease in the Vineyard with Strains of Xylella fastidiosa Benign to Grapevine. Plant Disease, 89(12), 1348-1352. https://doi.org/10.1094/PD-89-1348

Hopkins, D. L., & Ager, K. L. (2021). Biological Control of Citrus Huanglongbing with EB92-1, a Benign Strain of Xylella fastidiosa. Plant Disease, 105(10), 2914-2918. https://doi.org/10.1094/PDIS-02-21-0362-RE

Johnson, K. A., Bock, C. H., & Brannen, P. M. (2021). Phony peach disease: past and present impact on the peach industry in the southeastern U.S.A. CABI Agric Biosci, 2, 29. https://doi.org/10.1186/s43170-021-00049-4

Killiny, N., & Almeida, R. P. P. (2009). Host structural carbohydrate induces vector transmission of a bacterial plant pathogen. Proceedings of the National Academy of Sciences, 106(52), 22416-22420. https://doi.org/10.1073/pnas.0908562106

Newman, K. L., Almeida, R. P. P., Purcell, A. H., & Lindow, S. E. (2004). Cell-cell signaling controls Xylella fastidiosa interactions with both insects and plants. Proceedings of the National Academy of Sciences, 101(6), 1737-1742.

Pande, S., Shitut, S., Freund, L., Westermann, M., Bertels, F., Colesie, C., Bischofs, I. B., & Kost, C. (2016). Metabolic cross-feeding via intercellular nanotubes among bacteria. Nature Communications, 6, 6238.

Rashed, A., Killiny, N., Kwan, J., et al. (2011). Background matching behaviour and pathogen acquisition: plant site preference does not predict the bacterial acquisition efficiency of vectors. Arthropod-Plant Interactions, 5, 97–106. https://doi.org/10.1007/s11829-010-9118-z

Rapicavoli, J., Ingel, B., Blanco-Ulate, B., Cantu, D., & Roper, C. (2018). Xylella fastidiosa: an examination of a re-emerging plant pathogen. Molecular Plant Pathology, 19, 786-800. https://doi.org/10.1111/mpp.12585

Trkulja, V., Tomić, A., Iličić, R., Nožinić, M., & Milovanović, T. P. (2022). Xylella fastidiosa in Europe: From the Introduction to the Current Status. Plant Pathology Journal, 38(6), 551-571. https://doi.org/10.5423/PPJ.RW.09.2022.0127

Van Sluys, M., De Oliveira, M., Monteiro-Vitorello, C., Miyaki, C., Furlan, L., Camargo, L., Da Silva, A., Moon, D., Takita, M., & Lemos, E. (2003). Comparative analyses of the complete genome sequences of Pierce's disease and citrus variegated chlorosis strains of Xylella fastidiosa. Journal of Bacteriology, 185(3), 1018-1026.

Vandenkoornhuyse, P., Quaiser, A., Duhamel, M., Le Van, A., & Dufresne, A. (2015). The importance of the microbiome of the plant holobiont. New Phytologist, 206(4), 1196-1206.

Wei, Z., Gu, Y., Friman, V. P., Kowalchuk, G. A., Xu, Y., Shen, Q., & Jousset, A. (2019). Initial soil microbiome composition and functioning predetermine future plant health. Science Advances, 5(8), eaaw0759.

Wu, L., Cao, Z., Hu, Z., Chen, Y., Zhao, J., Wang, M., Guo, H., & Liu, X. (2021). Nonpathogenic Xanthomonas oryzae reduces pathogen infection and promotes plant growth in greenhouse pot experiments. Plant Disease, 105(7), 2030-2037. https://doi.org/10.1094/PDIS-02-21-0362-RE

Zhang, S., Flores-Cruz, Z., Kumar, D., Chakrabarty, P., Hopkins, D. L., & Gabriel, D. W. (2011). The Xylella fastidiosa Biocontrol Strain EB92-1 Genome Is Very Similar and Syntenic to Pierce's Disease Strains. Journal of Bacteriology, 193(3). https://doi.org/10.1128/jb.05430-11

NIS-Elements (RRID:SCR_014329)

CHAPTER 3

Virulence Evolution Via Pleiotropy in Insect-Vectored Plant Pathosystems

3.1 ABSTRACT

The dynamics and determinants of virulence evolution in insect-vectored plant pathosystems are complex and poorly understood. Here we use individual-based simulations to investigate how virulence evolution depends on genetic trade-offs and population structure in pathogen populations. Although quite generic, the model was inspired by the ecology of the plant-pathogenic bacterium *Xylella fastidiosa*, and we use it to gain insight into the evolution of virulence in that group. We find that even when pathogens find themselves much more often in hosts than vectors, selection in the vector environment can indeed cause correlational and non-adaptive changes in virulence in the host. The extent on such correlational virulence evolution depends on many system parameters, including the transmission rate, the strength of pleiotropy, the proportion of the population occurring in hosts versus vectors, the strengths of selection in host and vector environments, and the extent of virulence.

3.2 INTRODUCTION

The theory of virulence evolution is based on pathogen life history trade-offs. It predicts an optimal level of virulence that balances short- and long-term transmission efficiency (Anderson & May 1982; Ewald 1983; Frank 1996). In general, short-term transmission efficiency increases with within-host pathogen density. But high pathogen density within a host causes virulence, that is, excess host mortality. This shrinks the temporal window in which an infected host can be the source for pathogen transmission to a new host. Thus, virulence evolution entails a meta-population-level negative feedback. A pathosystem's

optimal level of virulence is the one that maximizes pathogen transmission over the long-term (Porco et al. 2005).

The classical trade-off theory is based on the epidemiological compartment models that are not explicitly population genetic (Gomez et al. 2020). They tell us about equilibrium conditions, that is, where a system is ultimately headed given a fixed set of ecological parameters. But they tell us nothing about how long a system might take to arrive at equilibrium conditions, or what might happen along the way (Day et al. 2004). Moreover, since epidemiological compartment models do not explicitly consider the genetic architectures of pathogen traits mediating virulence – or assume very simple monogenic, bi-allelic architectures – they tell us nothing about how the evolution of virulence might depend on variation in its genetic architecture. Nevertheless, certain genetic architectures could have strong impacts on how virulence evolves to its optimum.

To make all this a little more concrete, consider the case of virulence evolution in the plant-pathogenic bacterium *Xylella fastidiosa,* which is xylem-limited and insect-vectored, that is, occurs in two types of environments: the xylem vessels of its host plants, or the mouths of its xylem-consuming insect vectors. *X fastidiosa* is associated with a wide range of host species (Rapicavoli et al. 2017). In most cases it is a benign commensalist, but in some cases, infections are highly virulent, and *X. fastidiosa* is the causative agent of several important agricultural diseases, such as phony peach disease (Johnson et al. 2021), Olive Quick Decline Syndrome (Trkulja et al. 2022, Rapicavoli et al. 2017), and Pierce's disease in grapevine (Rapicavoli et al. 2017). The emergence of the latter in California was co-incident with the spread of a new vector species, the glassy-winged sharpshooter (Hemiptera: Cicadellidae*: Homalodisca vitripennis*). In comparison to many resident species of xylem-consuming insects, *H. vitripennis* is an exceptionally inefficient vector (Bextine 2006, Redak 2004). But as it established in California, it became so numerically dominant that most transmission to and from grapevine in California is now

via *H. vitripennis.* Could it be that the evolution of increased virulence of *X. fastidiosa* on grapevine was a non-adaptive correlational response to strong selection on traits that increased transmission efficiency in *H. vitripennis*?

In fact, there are other many cases in which the emergence of high-virulence pathogen genotypes is associated with the emergence of a new vector species or genotype. For example, the global spread of the *Bemisia tabaci* is thought to have driven extensive divergence and multiple independent cases of virulence evolution in begomoviruses, which now cause serious diseases problems in crops ranging from okra in western Africa to tomato in Peru and Taiwan (reviewed by Gilbertson et al. 2015).

Nevertheless, in a heterogeneous environment, selection tends to be more efficient in habitat types that are more common or productive (Whitlock 1996; Via and Lande 1985; Draghi 2023), and in insect-vectored plant pathosystems, the host environment is much more common and productive than the vector environment. Thus, we might expect the evolution of virulence-affecting pathogen phenotypes to be driven by selection in the host environment, with evolutionary change in the vector being largely correlational until the pathogen population has gotten close to the adaptive optimum in the host (Via and Lande 1985). And we might doubt the possibility of selection for increased performance in vectors driving the evolution of virulence in hosts. On the other hand, the evolution of high virulence in pathogens – which kills hosts – could effectively reduce disparities in the relative abundance and productivity of hosts versus vectors. And in a vector-borne pathosystem, the habitat variation experienced by parasite genotypes is largely of the course-grained temporal variety; transmission entails obligate, and asynchronous alternations between host and vector environments. How such a life history affects asymmetries in selection across habitat types is not clear. Does it entirely erase the effects of asymmetries in the abundance and productivity of different habitat types? Does it reduce them to disparities in the sway of neutral processes such as genetic drift? Or does

something more complex and nuanced happen? Here, to improve our intuition about how genetic architecture and environmental heterogeneity interact to shape the course of the evolution of virulence, we develop and analyze an individual-based simulation model.

3.3 METHODS

Simulations were performed with SLiM 4 (Haller & Messer, 2022). SLiM runs forward-time, individual-based, population genetic models. SLiM models are specified with codes written in the Eidos language. The Eidos code for the model described here is provided in Appendix 1.

To reiterate, our main research questions are about how the evolution of virulence may depend on pathogen population structure and genetic trade-offs affecting pathogen phenotypes in host and vector environments. Thus, they are quite general. Nevertheless, our motivation for developing the model was to gain insights into the evolution of virulence in *X. fastidiosa*, and so some decisions about model parameterization were made so as to approximate *X. fastidiosa* pathosystems.

Parameter Symbols	Parameter Definitions	Range of Parameter Values
k	Strength of pleiotropic covariance	-0.9 – 0.9
ωv	strength of vector selection	1 – 10
ωh	strength of host selection	1 -10
mr	migration rate	0.001 - 0.2
Hm	rate of host mortality	0.0001 - 0.01
V_{max}	maximum virulence effect	0.01 - 0.8
K_h	host carrying capacity	200 – 2000
K_v	vector carrying capacity	10 – 100
ρ	proportion of hosts	0.1 - 0.5
Variable Symbols	**Variable Definitions**	**Range of Variable Values**
T	How many generations it takes to evolve a mean host-performance phenotype within 10% of the optimum	201 – 10,000
Γ	Measure of the degree to which the population's evolutionary path bends towards the optimum in the vector or host environment	-2.0 – 2.0

Table 3.1: On top - Model parameter definitions along with the range of values explored. On bottom – model variable definitions and domains.

We simulated the evolution of a structured meta-population of pathogen individuals, each of which has a diploid, single-chromosome, 40kb genome. To be clear, these details about the genomic architecture are arbitrary and should not affect our inferences. Individuals in the simulations reproduce clonally and without recombination, and there are no dominance interactions between alleles. Hence, the genome is essentially a container for mutations, and should function equivalently to a haploid, circular genome of twice the size. That would still be much smaller than the genomes of *Xylella fastidiosa* (Simpson et al. 2000), but the mutation rate in the simulation is much higher. Again, our intention is to gain insights into the general causes of virulence evolution, not to parameterize a model in strict accordance with *Xylella* pathosystems.

At the start of each simulation, the population is genetically uniform. The pathogen population is divided into N_d=100 demes, each of which occurs in either a host or vector individual. So as not to be confused with pathogen individuals, we refer to these as two kinds of habitat patches. We let the proportion of host patches to vector patches, ρ, vary across simulations {0.1-0.5}. Below, we focus on our discussion on simulations in which ρ = 0.1.

This is not a multi-species model; we assume that host and vector habitats are fixed during a simulation. That being said, we do allow for turnover of vector and host patches. In each pathogen generation, each pathogen deme runs the risk of extinction, at background mortality rates μ_v {0.05} in vector patches and and mu_h {0.0001 – 0.01} in host patches. In hosts, this background rate can be elevated by a virulence effect. Specifically, $v_i = v_{max} / (1 + \exp(-a*d_i))$, where v_i is the excess risk of mortality experience by host i, v_{max} is the maximum possible virulence effect {0.01 – 0.8}, d_i is the density of pathogens within host i, that is n_i/K_i, and a=5 controls the steepness of the logistic mapping of pathogen density to virulence. Patch replacement is instantaneous. When vector or host dies, the number of

pathogens in that particular patch is set to zero. The patch is then immediately available for re-colonization in the next pathogen generation.

The pathogen life cycle begins with offspring production. Reproduction is clonal, with each surviving individual producing one offspring individual. Generations are overlapping. Offspring genomes are generated by random mutation of the parental genome. The mutation rate is 1e-8 per site, per genome, per generation. When a mutation occurs, a two-dimensional vector of allele effects is drawn from a zero-meaned random bivariate normal distribution with variances of 1.0, and symmetrical covariances, k, the sign and magnitude of which controls the pleiotropy between two pathogen quantitative phenotypes. An individual's host-performance phenotype is determined by the sum of the first elements of allele effect vectors. Likewise, an individual's vector-performance phenotype is the sum of the second elements of allele effect vectors. So, if $k > 0$, positive pleiotropy prevails and an allele that increase the host-performance phenotype value tends to also increase the vector-performance phenotype value. Conversely, when $k < 0$, antagonistic pleiotropy prevails. Here our main goal is to get a sense for how antagonistic pleiotropy between phenotypes affecting performance in vectors and hosts might drive the evolution of virulence. Therefore, we focus on models in which k=-0.8. But we also consider a range of other values {-0.9 – 0.9}.

The next step in the life cycle is migration. This happens at per capita rate mr {0.001 - 0.2} and is random between patches except for the constraint that migrants from a host patch can only move to a vector patch and vice versa. In an alternative version of the model, we relax this constraint and let migration be completely random between patches. In other words, we do away with vector transmission, and consider the evolution of a population in an environment in which there are two kinds of hosts, one being large, rare and susceptible to infection, and the other being small, abundant and tolerant of infection. By comparing pathogen evolutionary dynamics in this system to the main vector-born model, we can

zero in on the effects of vector-based transmission. For an example of population setups in the main and alternative versions of the model, see Fig. 3.1.

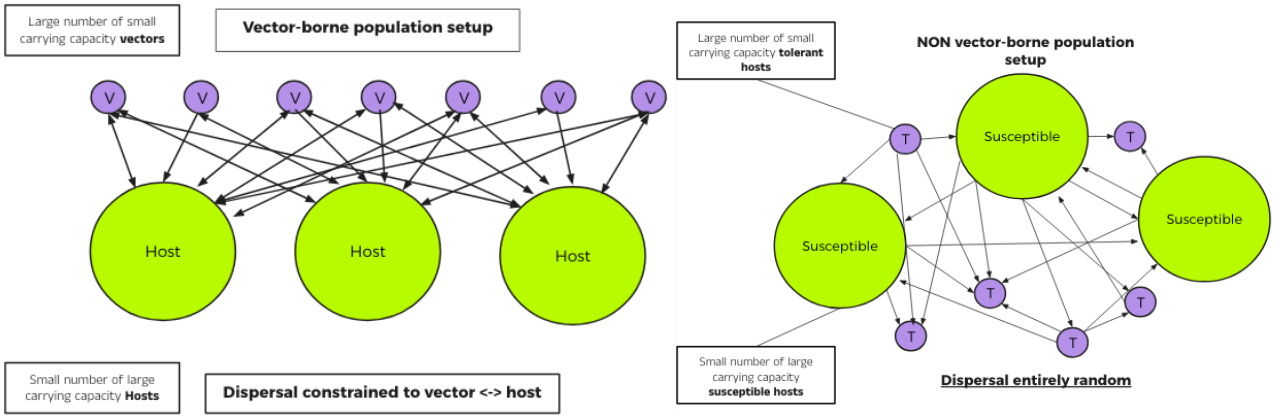

Fig. 3.1: A visual example of each type of population setup used in our simulations. On the left, the main model version in which migration of individuals is constrained to only occur from vector to host and vice versa, to mimic a vector borne transmission system. On the right, the alternative model version, in which migration is entirely random between resource patches.

After migration comes selection and population regulation. This entails genotype-environment matching, and density dependence. In the vector environment, the match between a pathogen's vector performance phenotype and the local optimum, determines their viability, that is, their survival probability. This matching is via a standard Gaussian fitness function, with variance ω_v {1.0-10.0} setting the weakness of selection. In the host environment, viability is the output of the same kind of Gaussian fitness function, but with variance ω_h {1.0-10.0}. Thus, we can examine how the evolution of the pathogen population depends on the absolute and relative strengths of selection in host and vector environments. In vector and host patches, individual-level fitness is also density dependent; in patch *i*, each individual's viability is rescaled by the ratio of the patch

carrying capacity K_i and the current pathogen population size, n_i. As mentioned above, in the host, there is also group-level selection via a virulence effect. As populations evolve mean host-performance phenotype values that more closely match the optimal value for the host environment and their within-host fitness increases, so too does the rate of host death, that is, deme extirpation. Note that selection is hard; it affects survival and thus has demographic effects.

After selection, the life cycle starts again with offspring production.

At the start of each simulation, pathogens are monomorphic, with a value of zero for their vector-performance and host-performance phenotypes, and the optimal value for each of these phenotypes is set to 5.0 phenotypic units. During the first 200 generations, the pathogen population is subject only to density-dependent regulation; selection and virulence effects are not applied, and so genetic diversity accumulates. Then, starting at generation 201, selection and virulence commence.

Our view of how the population approaches the phenotypic optima in host and vector habitats is based on two test statistics. The first, *T,* is simply how many generations it takes to evolve a mean host-performance phenotype within 10% of the optimum, and thus closely approach their maximum virulence effect on the host. Note that because of the negative meta-population-level feed-backs induced by high virulence, such proximity to the optimum host value might not be adaptive for the pathogen population; in other words, a mean host-performance phenotype value within 10% of the optimum might not the equilibrium state of a pathosystem. So, *T* is best interpreted as the hazard of evolving high virulence, even if only temporarily.

The second statistic we track, Γ, is a measure of the degree to which, until the 10% phenotype-host-environment threshold is hit, the population's evolutionary path bends

towards the optimum in the vector or host environment. In other words, we look at the extent to which adaptive responses in the pathogen population are dominated by the vector or host habitat types (See Fig 3.2 for an example).

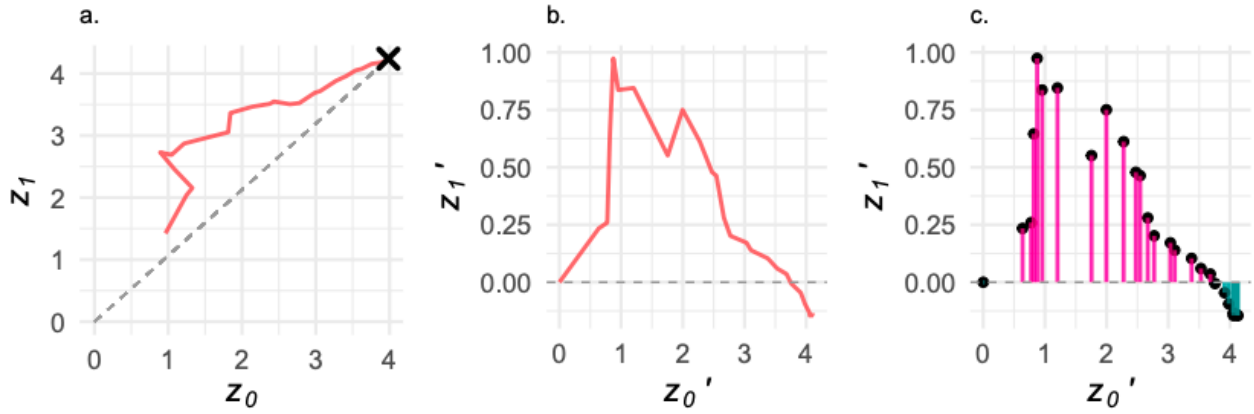

Fig. 3.2: Calculation of the Γ statistic. (a) An example evolutionary path through the phenotype space. For this simulation k=-0.2, v_{max}=0.3, mr=0.1, K_v=20, K_h=2000, ω_v=3.0, ω_h=3.0, m_h = 0.0001, m_v=0.1, and ρ = 0.1. (b) That same path translated to start at the origin and rotated so that the ideal path from the origin to the joint phenotypic optimum lies along the x-axis. (c) Γ is calculated as the sum of deviations from the ideal path, scaled by the length of the path in generations.

To calculate Γ (the deviation from the ideal evolutionary path) we use trigonometry. First, we translate a population's evolutionary path through the phenotypic space so as to start at the origin. We do this by subtracting the first post-burnin (generation 201) mean value for each phenotype (z_0, and z_1) from the mean phenotype value for each subsequent generation. Since the optimal value for each phenotype is 5.0, and pathogen populations start out with phenotype values of 0.0, a straight evolutionary path to the joint optimal phenotype would have a slope of one. Therefore, for each simulation, we rotate the translated evolutionary path D radian degrees about the origin, where D is the inverse tangent of one. This rotation is done as follows: $z_{0i}' = z_{0i}*\cos(D) + z_{1i}*\sin(D)$; $z_{1i}' = z_{1i}*\cos(D) - z_{0i}*\sin(D)$, where (z_{0i}, z_{1i}) is point i along the simulated post-burnin translated evolutionary

path, z_{0i} is the population's mean value for the host performance phenotype, z_{1i} is the mean value for the vector performance phenotype, and (z_{0i}', z_{1i}') is that same point in the rotated coordinate space. We can then calculate the degree to which the evolutionary path bends towards what is optimal in the vector environment as sum(z_{1i}')/T, in other words, the per generation average deviation from the ideal evolutionary path.

To help parse and interpret what could be complex causal interactions among model parameters and variables we also keep track of the total pathogen population size occurring in hosts N_h, and vectors N_v.

A total of 200 simulations were performed for each version of the model, that is the vector-born transmission model, and the unfettered-migration model. For each run, a value for each free model parameter was drawn from a random uniform distribution with ranges as given in Table 3.1.

We analyzed simulation model outputs by fitting mutli-variate linear models, using both maximum likelihood-based and Bayesian interference methods (Burkner 2021). In one model, the response variable was log(T). In the other, the response was Γ. For both models the fixed predictor variables were ω_h, ω_v, ρ, mr, m_h, v_{max}, K_v, K_h, and the interactions ρ:K_h and ω_h:ω_v. Since there could be complex causal links in the system, we also analyzed model outputs by fitting structural equation models, using the R package *lavvan* (Rosseel et al. 2017). To make this more tractable, we replaced the terms for ρ and carrying capacities for hosts and vectors with the mean pathogen population size in each habitat type, N_h and N_v. As noted above, we focus on models in which pleiotropic covariances were strong and negative, that is, k=-0.8, and where vectors are more abundant than hosts, ρ=0.1, but have much smaller carrying capacities, and much higher mortality rates. But we also analyzed simulations in which these parameters were free to vary.

To sum up, we examined how (i) the time it takes a population to evolve a host-performance phenotype close to the optimal value, and (ii) the degree to which a population's evolution path through the phenotypic space bends towards either vector or host environments depends on (a) the relative abundance of host and vector patches, (b) the relative carrying capacities of host and vector demes, (c) the relative strengths of selection in host and vector demes, (d) the migration rate, and (e) the maximum virulence effect of high density in host demes. We also considered how all of this is affected by doing-away with vector-based transmission and allowing for completely random migration.

3.4 RESULTS AND DISCUSSION

Let us start by considering the linear model of the variance in log(T), when k=-0.8 and ρ=0.1 and there is vector-based transmission. In this model, the predictors explained about half of the variance in log(T) (adjusted-R^2 = 0.5). All effects are expressed in units of standard deviations.

3.4.1 Log(T)

Two parameters significantly decrease log(T), that is the time it takes for close adaptation to the host environment optimum. The first is ρ, that is, the proportion of host patches to vector patches (coefficient = -3.5 SD, p-value = 0.012). The second is K_h, that is the carrying capacity of each host patch (coefficient = -9.7e-4; p-value = 0.015). But there is a significant interaction between those parameters; as K_h increases, the negative effect on log(T) is diminished. This is intuitive; both parameters increase the total share of the pathogen population that occurs in host patches, and thus a decrease in one parameter value can be compensated for by an increase in the other. The sign and significance of these effects would seem to support the hypothesis that even with course-grained

temporal habitat variation, selection tends to be more efficient in a particular habitat when it is more common (Whitlock 1996; Draghi 2023). Recall that because of negative meta-population-level feed-backs a close match between the mean host-performance phenotype and the optimum can be nonadaptive. In that case, hitting the host-habitat-match threshold could be largely dictated by neutral or correlational evolutionary processes. But as the total size of the pathogen population found within the host environment increases, the odds of high virulence evolving via drift would seem to shrink. Moreover, as K_h and ρ increase, we expect the balance between within-host and meta-population-level selection to shift more to within-host, and thus the evolutionarily stable strategy to shift to a closer match to the host optimum. Nevertheless, virulence effects certainly complicate the interpretation of variance in T, and therefore our alternative statistic Γ, is especially useful.

Three parameters significantly increase log(T). First, we have v_{max}, the maximum additional host mortality than can be caused by an infection (coefficient = 2.9, p-value = <2e-16). This is as expected; as v_{max} rises, so does the meta-population-level fitness cost of evolving a within-host performance phenotype that closes matches the optimum; the negative feedback on virulence evolution increases in strength. The variable log(T) also tends to increase with larger values for ω_h, that is, with weaker selection in host patches (coefficient = 0.2; p-value < 2-e16), and this is also as expected. Simply put, adaptation to the host environment is slower when the within-host fitness consequences of maladaptation are less pronounced. The third significant effect is less intuitive; log(T) increases with weakening selection in vectors (coefficient = 0.09; p-value = 3.1e-4), although this effect is several orders of magnitude weaker than the effect of weakening selection in the host environment. At first blush, one might predict that with strong negative pleiotropies, weakening selection in the vector should increase the efficiency of selection in the host. But that would be to ignore the potential demographic effects of weaker selection in vectors. We suspected that since selection is hard, by weakening

selection in the vector, we might effectively increase the average proportion of the pathogen population that can survive in vector patches, and that this demographic effect would slow down adaptation to the host by increasing the odds of a particular genotype being exposed to habitat heterogeneity.

Next, let us turn to the linear model of the variance in Γ, that is, the degree to which simulated evolutionary paths are dominated by the vector environment.

3.4.2 Gamma

Two parameters significantly increase Γ (the deviation from the ideal evolutionary path). The first is ω_h (coefficient = 0.53, p-value < 2e-16); the evolution of simulated pathogen populations is dominated more by selection in the vector environment when selection in the host is weaker. The variable Γ is also positively correlated with v_{max} (coefficient = 0.64; p-value < 2e-16). This is consistent with our interpretation of the model decomposing variance in log(T); increasing the negative feedback on adaptation to the host environment should increase the relative efficiency of selection in vectors. On the other hand, two parameters significantly decrease Γ: migration rate (coefficient = -0.12; p-value = 1.9e-4), and ω_v (coefficient = -0.23; p-value = 2.14e-11). As one might expect, weakening selection in the vector environment reduces the extent to which it bends a population's evolutionary path. As for the migration effect, much classical theory (Eshelman et al. 2010) suggests that increasing migration rate can attenuate meta-population-level fitness cost of virulence, and thereby reduce the negative feed-backs that interfere with adaptation to the host environment.

Now, let us put it all together with a structural equation model (Fig 3.3.).

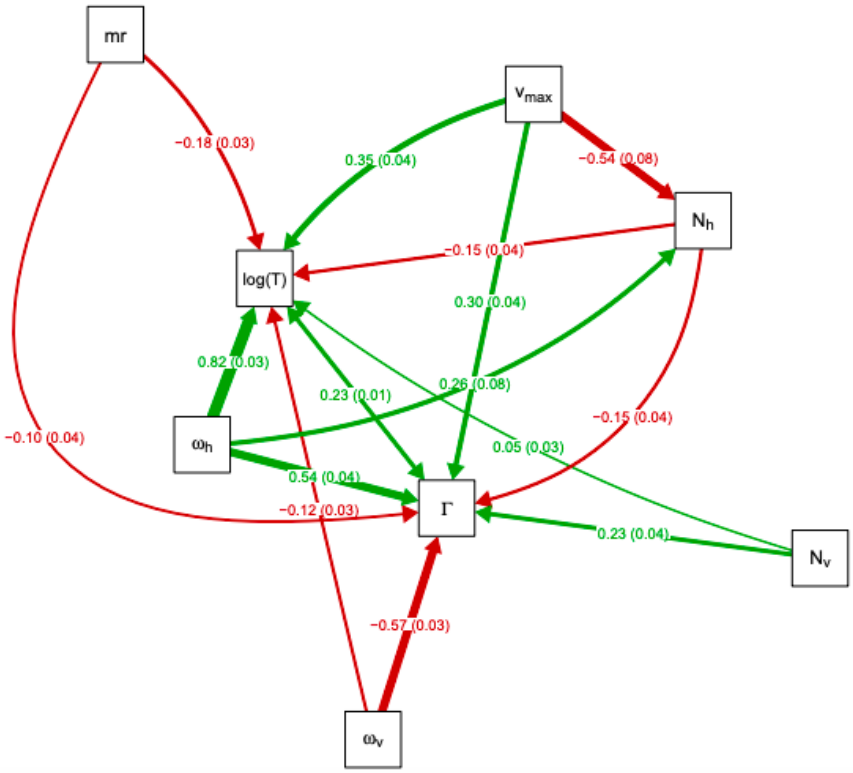

Response Variables:

- Γ - Deviation from the ideal evolutionary path
- log(T) - log adjusted time value

Parameters:

- N***v*** - number of individuals in vector populations
- Nh- number of individuals in host populations
- GƟh - Strength of host selection
- GƟv - Strength of vector selection
- Mr - migration rate
- Vmax - maximum virulence effect

Fig. 3.3: Structural equation model of the vector borne pathogen population setup. Values in units of effect and standard deviation, and the thickness of the lines corresponds to the level of effect the parameter had on another parameter or response variable.

Can selection in vectors on antagonistically pleiotropic loci affect correlational and potentially non-adaptive evolution of virulence in the host? The structured equation model suggests that it is possible. Weakening selection in the vector significantly reduces log(*T*) (coefficient = -0.12; p-value < 1e-4) and *Γ* (coefficient = -0.57; p-value < 1e-4). Conversely, weakening selection in the host environment tends to increase log(*T*) (coefficient = 0.82; p-value < 1e-4) and *Γ* (coefficient = 0.54; p-value < 1e-4). But the frequency at which

pathogen genotypes encounter host or vector environments is also important; Larger values for N_h tend to reduce log(T) (coefficient = -0.15; p-value < 1e-4) and Γ (coefficient = -0.15; p-value < 1e-4). Meanwhile, increasing the total number of pathogens in vectors, N_v increases Γ and log(T), although the latter effect is not significant. So, the structural equation models is telling us that habitat type frequency (i.e. the values for N_h and N_v) certainly has a powerful effect on the evolution of the pathogen population, as per the classical theoretical work of Whitlock (1996) and others, but these effects are of a smaller magnitude than the strength of selection in each habitat type, and selection in vectors is just about as important as selection in hosts.

The evolution of virulence in hosts also depends strongly on pathogen transmission rate, mr, and the upper limit of the virulence effect, v_{max}. Transmission rate has a negative effect on log(T) (coefficient = -0.18; p-value < 1e-4), and a positive effect on Γ (coefficient = 0.10; p-value = 0.021). Previous theoretical work has shown that in simple pathosystems, the optimal level of virulence increases with pathogen transmission rate (Porco et al. 2005); this likely explains the negative effect of mr on log(T) and Γ – since it makes a close match between the host-performance phenotype and the optimum value more adaptive. Before fitting the model, we hypothesized that the v_{max} parameter could affect pathogen evolution in two ways. It could affect log(T) and Γ directly by changing the adaptive landscape, to wit, by reducing the maximum productivity of host patches. Or it could affect log(T) and Γ indirectly, by reducing N_h. The model shows that both are important; v_{max} has a strong negative effect on N_h (coefficient = -0.81; p-value < 1e-4) as well as strong positive direct effects on log(T) and Γ. (coefficient for log(T) = 0.35; p-value < 1e-4; coefficient for Γ = 0.26; p-value < 1e-4).

3.4.3 Non-vector borne simulations

To get a better sense for the importance of vector-based transmission, we also ran simulations in which pathogen migration was completely random. We put this together with a structural equation model as well (see Fig 3.4)

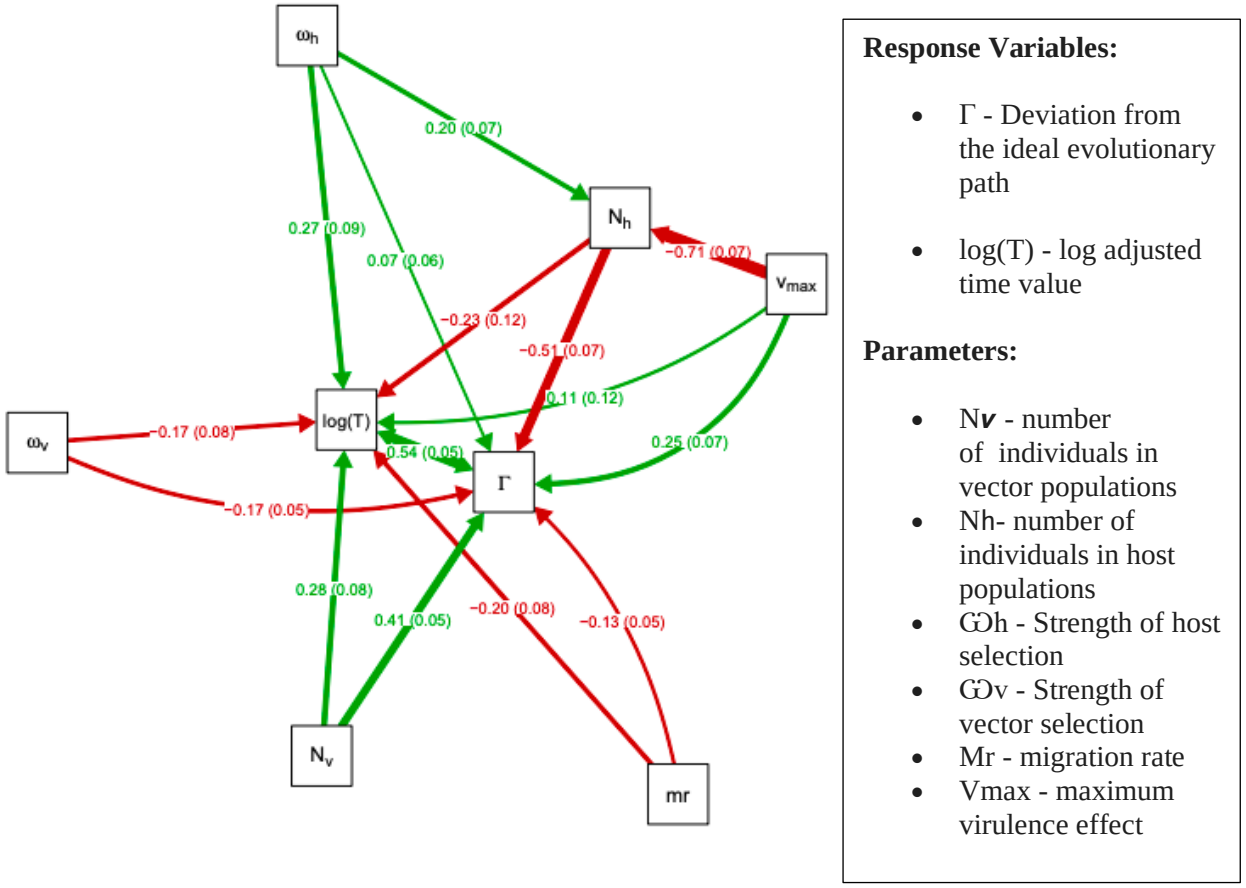

Figure 3.4: structural equation model of the non-vector-borne pathogen population setup. Values are in units of effect and standard deviation, and the thickness of the lines corresponds to the level of effect the parameter had on another parameter or response variable.

As mentioned above, in this case, the model is better interpreted as one of the evolution of a pathogen population in an environment composed of a mix of susceptible and tolerant hosts. Comparison of the two SEMs indicates that the effects of vector-born transmission are rather subtle, entailing changes in the specific weights but not the signs of causal interactions. Without vector-based transmission, the effects of the weakness of selection in each type of habitat on both log(T) and Γ are attenuated. The same is true of the direct effects of v_{max}, although its indirect effects via the size of the pathogen population in the susceptible host type is stronger. In all, it appears that vector-born transmission tends to increase the importance of divergent selection between habitat types, and somewhat decrease the importance of demographic disparities between habitat types.

3.5 CONCLUSIONS

Let us close by reconsidering the evolution of virulence in *Xylella fastidiosa*. In California vineyards, the emergence of new highly virulent genotypes closely followed the establishment of a new, markedly inefficient vector species. To reiterate, similar sequences of vector turnover and virulence evolution have been found in other pathosystems, in particular those involving the whitefly species *B. tabaci* (Gilbertson et al. 2015). Could this have been because of negative genetic correlations between traits affecting performance in vectors and hosts? Our simulation model suggests the answer is yes, possibly. Strong selection for improved performance in the vector can in fact cause correlational evolution of pleiotropic host-performance traits. In theory this could also arise via tight linkage rather than pleiotropy per se, although we did not investigate that here (Via and Lande 1985). Moreover, if such correlational evolution in the host causes a non-adaptive increase in virulence, that is increase v_{max}, the demographic consequences could further bend the evolutionary path towards the vector optimum. And this could slow down fitness optimization in the host.

Of course, using this hypothesis to explain the evolution of virulence in *Xylella* presupposes that there are some strong antagonistic pleiotropies affecting performance in hosts and vectors. But this could be. Indeed, much of the virulence of *Xylella* infections has been attributed to the plastic induction of "sticky" cell phenotypes which ultimately clog xylem vessels, but which also increase the efficiency of acquisition by vectors (Kyrkou et al. 2018). Of course, there are other tenable hypotheses for the evolution of increased virulence in *X. fastidiosa* in Californian vineyards. In particular, in addition to be an especially poor vector, *H. vitripennis* is an exceptionally polyphagous vector. And so, the story of virulence evolution in Californian populations of *X. fastidiosa* likely also entails changes their population structure, perhaps increasing the alpha diversity of pathogen communities and the potential for phenotypic evolution via recombination (many examples of which can be found in Gilbertson et al. 2015). Nevertheless, we cannot yet reject the maladaptive correlational evolution hypothesis.

3.6 REFERENCES

Alizon S, Hurford A, Mideo N, Van Baalen M. Virulence evolution and the trade-off hypothesis: history, current state of affairs and the future. J Evol Biol. 2009 Feb;22(2):245-59. doi: 10.1111/j.1420-9101.2008.01658.x. PMID: 19196383.

Anderson RM, May RM. Directly transmitted infections diseases: control by vaccination. Science. 1982 Feb 26;215(4536):1053-60. doi: 10.1126/science.7063839. PMID: 7063839.

Bextine, Blake, Brian C Jackson, and Matthew J Blua. Quantitative aspects of the transmission of xylella fastidiosa by the ..., 2006. https://static.cdfa.ca.gov/PiercesDisease/proceedings/2006/2006_13-17.pdf.

Bürkner P (2017). "brms: An R Package for Bayesian Multilevel Models Using Stan." Journal of Statistical Software, 80(1), 1–28. doi:10.18637/jss.v080.i01.

Bürkner P (2018). "Advanced Bayesian Multilevel Modeling with the R Package brms." The R Journal, 10(1), 395–411. doi:10.32614/RJ-2018-017.

Bürkner P (2021). "Bayesian Item Response Modeling in R with brms and Stan." Journal of Statistical Software, 100(5), 1–54. doi:10.18637/jss.v100.i05.

CDFA. Pierce's Disease Control Program State Miscellaneous ruling, March 10, 2020. https://pi.cdfa.ca.gov/pqm/manual/pdf/454.pdf.

Cressler CE, McLEOD DV, Rozins C, VAN DEN Hoogen J, Day T. The adaptive evolution of virulence: a review of theoretical predictions and empirical tests. Parasitology. 2016 Jun;143(7):915-930. doi: 10.1017/S003118201500092X. Epub 2015 Aug 25. PMID: 26302775; PMCID: PMC4873896.

Ebert D, Mangin KL. THE INFLUENCE OF HOST DEMOGRAPHY ON THE EVOLUTION OF VIRULENCE OF A MICROSPORIDIAN GUT PARASITE. Evolution. 1997 Dec;51(6):1828-1837. doi: 10.1111/j.1558-5646.1997.tb05106.x. PMID: 28565099.

Ebert, 1994. Evolution of infectious disease. Oxford University Press, New York, New York, 298 p.

Eshelman CM, Vouk R, Stewart JL, Halsne E, Lindsey HA, Schneider S, Gualu M, Dean AM, Kerr B. Unrestricted migration favours virulent pathogens in experimental metapopulations: evolutionary genetics of a rapacious life history. Philos Trans R Soc Lond B Biol Sci. 2010 Aug 27;365(1552):2503-13. doi: 10.1098/rstb.2010.0066. PMID: 20643740; PMCID: PMC2935104.

Frank SA. Models of parasite virulence. Q Rev Biol. 1996 Mar;71(1):37-78. doi: 10.1086/419267. PMID: 8919665.

Fenner, F, Ratcliffe, F. N. (1965). Myxomatosis. Cambridge University Press (in the Press).

Froissart R, Doumayrou J, Vuillaume F, Alizon S, Michalakis Y. The virulence-transmission trade-off in vector-borne plant viruses: a review of (non-)existing studies. Philos Trans R Soc Lond B Biol Sci. 2010 Jun 27;365(1548):1907-18. doi: 10.1098/rstb.2010.0068. PMID: 20478886; PMCID: PMC2880117.

Gilbertson RL, Batuman O, Webster CG, Adkins S. Role of the Insect Supervectors Bemisia tabaci and Frankliniella occidentalis in the Emergence and Global Spread of Plant Viruses. Annu Rev Virol. 2015 Nov;2(1):67-93. doi: 10.1146/annurev-virology-031413-085410. PMID: 26958907.

Glassy-winged sharpshooter management guidelines--UC IPM - ucanr.edu. Accessed January, 11, 2024. https://ipm.ucanr.edu/PMG/PESTNOTES/pn7492.html.

Gomez LM, Meszaros VA, Turner WC, Ogbunugafor CB. The Epidemiological Signature of Pathogen Populations That Vary in the Relationship between Free-Living Parasite Survival and Virulence. Viruses. 2020 Sep 22;12(9):1055. doi: 10.3390/v12091055. PMID: 32971954; PMCID: PMC7551987.

Host-Parasite Relations, Vectors, and the Evolution of Disease Severity P W Ewald Annual Review of Ecology and Systematics 1983 14:1, 465-485

Kyrkou I, Pusa T, Ellegaard-Jensen L, Sagot MF, Hansen LH. Pierce's Disease of Grapevines: A Review of Control Strategies and an Outline of an Epidemiological Model. Front Microbiol. 2018 Sep 12;9:2141. doi: 10.3389/fmicb.2018.02141. PMID: 30258423; PMCID: PMC6143690.

Levin BR. The evolution and maintenance of virulence in microparasites. Emerg Infect Dis. 1996 Apr-Jun;2(2):93-102. doi: 10.3201/eid0202.960203. PMID: 8903208; PMCID: PMC2639826.

Levin BR, Svanborg Edén C. Selection and evolution of virulence in bacteria: an ecumenical excur-sion and modest suggestion. Parasitology. 1990;100 Suppl:S103-15. doi: 10.1017/s0031182000073054. PMID: 2235060.

Messenger SL, Molineux IJ, Bull JJ. Virulence evolution in a virus obeys a trade-off. Proc Biol Sci. 1999 Feb 22;266(1417):397-404. doi: 10.1098/rspb.1999.0651. PMID: 10097397; PMCID: PMC1689683.

Porco TC, Lloyd-Smith JO, Gross KL, Galvani AP. The effect of treatment on pathogen virulence. J Theor Biol. 2005 Mar 7;233(1):91-102. doi: 10.1016/j.jtbi.2004.09.009. Epub 2004 Nov 13. PMID: 15615623; PMCID: PMC7126720.

Redak, R.A., Prucell, A.H., Lopes, J.R.S., Blua, M.J., Mizell III, R.F., and P.C. Andersen. 2004. The biology of xylem fluid-feeding insect vectors of Xylella fastidiosa and their relation to disease epidemiology. Annu. Rev. Entomol. 49:243-270.

Simpson, A., Reinach, F., Arruda, P. 2000. The genome sequence of the plant pathogen *Xylella fastidiosa*. *Nature* 406, 151–157 https://doi.org/10.1038/35018003

SLiM 4: Multispecies Eco-Evolutionary Modeling Benjamin C. Haller and Philipp W. Messer The American Naturalist 2023 201:5, E127-E139

Varela LG, Smith RJ, Phillips PA. 2001. Pierce's Disease. UC ANR Publication 21600. Oakland, CA.

Wilen CA, Hartin JS, Henry JM, Costa HS, Blua M, Purcell AH. April 2008. Pest Notes: Oleander Leaf Scorch. UC ANR Publication 7480. Oakland, CA

3.7 APPENDIX 1 (EIDOS CODE)

```
//This is a Non-Wright-Fisher model of the evolution of virulence via
//pleiotropy in a host-vector-parasite system

initialize() {
	initializeSLiMModelType("nonWF");
	initializeMutationRate(1e-8);
	initializeMutationType("m1", 0.5, "f", 0.0);
	initializeGenomicElementType("g1", m1, 1.0);
	initializeGenomicElement(g1, 0, 39999);
	initializeRecombinationRate(1e-8);
	defineConstant("mu", c(0.0, 0.0)); //[0.2] this was weird positive
	defineConstant("cov", cv);//-0.2
	defineConstant("sigma", matrix(c(1.0, cov,cov,1.0), nrow=2)); //the variance here is
1.0
	//defineConstant("MR", 0.05); //Migration Rate [0.15]
	defineConstant("vMax", vmx); // maximum virulence effect
	defineConstant("Host_Optima", 5.0);
	defineConstant("Vector_Optima", 5.0);
	defineConstant("MR", mra);
	//defineConstant("HK", hk);
	defineConstant("Run", ru); //you might want this later
	defineConstant("HK", hk); //Host carrying capacity [120,2000]
	defineConstant("VK", vk); //Vector carrying capacity [20]
	//defineConstant("VK", vk);
	//defineConstant("VS", 5.0); //strength of vector selection [HMMM... both of these
are pretty weak]
	defineConstant("VS", vs);
	//defineConstant("HS", 5.0);//strength of host selection
	defineConstant("HS", hs);
	defineConstant("HM", hm);
	//defineConstant("HM", 0.0001); //baseline host mortality
	defineConstant("VM", 0.05); //vector mortality [0.01] too low, changing to [0.05]
	defineConstant("Np", 100); //number of subpops [40,100]
	defineConstant("Ph", rho); //proportion of subpops that are hosts
	defineConstant("hostN", asInteger(Np*Ph));
	defineConstant("vectorN", Np - hostN);
	defineConstant("Vv", sv); //variation in optimum in vectors across cycles
}
```

```
reproduction() {
	subpop.addCloned(individual);
}

mutation(m1){
	Mutation_Effect= rmvnorm(1, mu, sigma); //draw from multivariate normal
	mut.setValue("e0", Mutation_Effect[0]); // set mutation effects (not sim effects)
	mut.setValue("e1", Mutation_Effect[1]);
	return T;
}

1 early(){
	//NEW METAPOP SETUP
	//first make the hosts
	//hostN = asInteger(Np * Ph);
	for (i in 1:hostN){
	  sim.addSubpop(i, HK);
	  sim.subpopulations[i-1].tag = 0;
	}
	//now do vectors
	//vectorN = Np - hostN;
	for (i in (hostN+1):Np){
	  sim.addSubpop(i, VK);
	  sim.subpopulations[i-1].tag = 1;
	}

	//NB: Since we don't ever change these things, it makes more sense for them to be
constants
	//sim.setValue("Host_Optima", 5); //HMMM. We placed this within closer reach.
Not sure that's right.
	//sim.setValue("Vector_Optima", 5); //[10] changed to 5 to match hosts
}

early(){
	allSubs = sim.subpopulations;
	hostSubs = allSubs[allSubs.tag == 0];
	vectorSubs = allSubs[allSubs.tag == 1];
	hostInds = hostSubs.individuals;
	vectorInds = vectorSubs.individuals;
	nHostMigrants = size(hostInds) ? rpois(1, size(hostInds)*MR) else 0;
	nVectorMigrants = size(vectorInds) ? rpois(1, size(vectorInds)*MR) else 0;
	hostMigrants = sample(hostInds, nHostMigrants);
```

```
        vectorMigrants = sample(vectorInds, nVectorMigrants);
        //DO MIGRATION

  for (migrant in hostMigrants){
    dest = sample(vectorSubs,1);
    dest.takeMigrants(migrant);
  }
  for (migrant in vectorMigrants){
    dest = sample(hostSubs,1);
    dest.takeMigrants(migrant);
  }
}

//add a burnin phase for the populaiton to grow some diversity
1:199 early(){
  allSubs = sim.subpopulations;
        hostSubs = allSubs[allSubs.tag == 0];
        vectorSubs = allSubs[allSubs.tag == 1];
  hostSubs.fitnessScaling = (HK / hostSubs.individualCount);
        vectorSubs.fitnessScaling = (VK / vectorSubs.individualCount);
}

//IN nonWF MODEL SELECTION NEEDS TO HAPPEN *EARLY* IN THE LIFE CYCLE
200: early(){
        inds = sim.subpopulations.individuals; // that's everyone
        //start by figuring out their phenotypes
        for (ind in inds){
                muts = ind.genomes.mutationsOfType(m1);
                Phenotype0 =  size(muts) ? sum(muts.getValue("e0")) else 0.0;
                Phenotype1 =  size(muts) ? sum(muts.getValue("e1")) else 0.0;
                ind.setValue("Phenotype0", Phenotype0);
                ind.setValue("Phenotype1", Phenotype1);
        }

        //do individual- and group-level fitness effects
        //NEEDED TO MAKE THIS WORK FOR ALL HOST AND VECTOR SUBPOPS
        allSubs = sim.subpopulations;
        hostSubs = allSubs[allSubs.tag == 0];
        vectorSubs = allSubs[allSubs.tag == 1];
        hostInds = hostSubs.individuals;
        vectorInds = vectorSubs.individuals;
```

```
	//FOR HOSTS
	//individual-level effects. viability increases with closer match between Phen0 and optimum
	MaxMatch1 = dnorm(0.0, 0.0, HS);
	//Host_Optima = sim.getValue("Host_Optima"); //DO WE CHANGE THIS? IF NOT MAKE A CONSTANT
	hop = Host_Optima + rnorm(1,0.0,Vv);
	host_devs = hop - hostInds.getValue("Phenotype0");
	Host_fit_effs = dnorm(host_devs, 0.0,  HS)/MaxMatch1;
	hostInds.fitnessScaling = Host_fit_effs;

	//group-level effects. but host patch mortality increases with parasite abundance
	//THESE NEXT TWO LINES WE DON'T USE ANYMORE, SINCE THINGS VARY ACROSS PATCHES
	//Host_MeanPh = mean(dnorm(Host_Optima - hostInds.getValue("Phenotype0"), 0.0,  HS))/MaxMatch1;
	//sim.setValue("Host_MeanPh", Host_MeanPh);

	//NEXT WE'VE GOT TO FIGURE HOST DEATH
	//WE WANT THIS TO WORK INDEPENDENTLY IN EACH HOST
	for (hsub in hostSubs){
	  if (size(hsub.individuals)){
	    //NB: I think it makes more sense to have virulence be a function of abundance
	    //rather than mean phen0 value
	    //phenMean = mean(hsub.individuals.getValue("Phenotype0"));
	    //phenMatch = dnorm(Host_Optima - phenMean, 0.0, HS)/MaxMatch1;

	    //So, we'll use a logistic function to convert pathogen density to excess death
	    density = size(hsub.individuals)/HK;
	    virulence = vMax/(1+exp(-5.0*density));

	    //pd = (HM + (1-phenMatch));
	    pd = HM + virulence;

	    a = rbinom(1, 1, pd);
	    if (a==1){ //then, we're killing the host
	        sim.killIndividuals(hsub.individuals);
	    }
	  }
	}

	//FOR VECTORS
```

```
        //individual-level effects
        MaxMatch2= dnorm(0.0, 0.0, VS);
        //Vector_Optima = sim.getValue("Vector_Optima");
        vop = Vector_Optima + rnorm(1,0.0,Vv);
        vec_devs = vop - vectorInds.getValue("Phenotype1");
        Vector_fit_effs = dnorm(vec_devs, 0.0,  VS)/MaxMatch2;
        vectorInds.fitnessScaling = Vector_fit_effs;
        //We need to use this to govern the the fitness of individuals in a vector
        sim.setValue("Vector_MeanPh", mean(vec_devs));

        //Vector extinction
        //HERE AGAIN WE HAVE TO GENERALIZE ACROSS ALL VECTORS
        //instead of a deterministic thing, where we kill the vector every X
        //generations, we'll just use a background extinction rate
        //We set this up in the initialization() callback
        for (vsub in vectorSubs){
          deathCoin = rbinom(1, 1, VM);
          if (deathCoin==1){
            sim.killIndividuals(vsub.individuals);
          }
        }
        //NOW DO THE DENSITY-DEPENDENT FITNESS SCALING
        hostSubs.fitnessScaling = (HK / hostSubs.individualCount);
        vectorSubs.fitnessScaling = (VK / vectorSubs.individualCount);
}

//JUST DO LOGGING LATE
200:10000 late(){
  inds = sim.subpopulations.individuals;
  //Host_Optima = sim.getValue("Host_Optima");
  //Let's do all of our writing to stdout here, just once every 100 cycles
  if (sim.cycle %10 == 0){
    mp0 = mean(inds.getValue("Phenotype0"));
    mp1 = mean(inds.getValue("Phenotype1"));
          catn("Gen: " + sim.cycle + " Mean phen0: " + mp0 + " | Mean phen1: " + mp1);
          writeFile("EndAllBeAll.csv",
paste(c(Run,cv,HS,VS,Ph,MR,HM,Vv,vMax,VK,HK,sim.cycle,mp0,mp1), sep=','),
append=T);

  }
          Host_Mean = size(inds) ? mean(inds.getValue("Phenotype0")) else 0.0;
          TheDeviation = abs(Host_Mean - Host_Optima);
```

```
	if (TheDeviation < (0.2 * Host_Optima)) {
		catn("Cycle: " + sim.cycle + " | The deviation: " + TheDeviation + " | The mean:
" +		Host_Mean);

		//writeFile("EndalltestCVPOP.csv",
paste(c(Run,HS,VS,Ph,MR,HM,sim.cycle), sep=','), append=T);

		sim.simulationFinished();
	}
}
```